

Topological phases in 1D, 2D and tight-binding models

A. Gómez Bañón

Universidad de Alicante, 03690 San Vicente del Raspeig, Spain

(Dated: December 20, 2019)

Our main goal in this report is to explore what we call *topological phases* in condensed matter physics. We develop the SSH and the Haldane model to exemplify different properties and consequences of topological order. We also find the tuning parameters of each model to produce topological phase transitions. The interpretation of the topological index as a winding number in the SSH model is also explained, and we make a numerical calculation of the Chern number for graphene.

I. MOTIVATION

The band structure of a system provides information to decide if a certain material is in an insulating or metallic phase. By tuning the different parameters of the Hamiltonian that describe such system, we can drive it across transitions between its possible phases. We are interested in the insulating phases that are said to be *topologically different*.

An insulating phase can be characterized by defining a *topological index*, analogous to the *genus* (g) of a manifold (M) in usual topology. In the case of condensed matter physics, the index is associated to a mapping between the \vec{k} points in the first Brillouin zone (BZ) and the possible Bloch states $|n(\vec{k})\rangle$ of an electron in the system.

More specifically, we will study Hamiltonians for tight-binding (abbreviated TB) models in 1D and 2D that can describe topologically different insulating phases. The dimensionality of the system plays a central role in the calculation of the topological index. For 1D systems, it is defined as:

$$W_n = \frac{1}{\pi} \oint_{BZ} dk \langle n(k) | i \frac{d}{dk} | n(k) \rangle \quad (1)$$

Where $n(k)$ denotes the n^{th} eigenstate of the Bloch Hamiltonian $H(k)$, for the k point in the first BZ (in this case, the BZ would be a periodic line segment). The integrand in (1) is the Berry connection¹ for the n^{th} energy band of a 1D system (the integral in (1) is the Berry phase¹ or Zak phase⁴). In the 2D case, we define the topological index as a surface integral over the BZ:

$$W_n = \frac{1}{2\pi} \int \int_{BZ} d^2k \cdot \vec{\Omega}_n \quad (2)$$

Where $\vec{\Omega}_n$ is the Berry curvature¹. For 2D systems, the quantity W_n is also called the 'Chern number'.

The connection with topology comes from the fact of having quantities (Berry connection and Berry curvature) that we can change locally by modifying system parameters (for example, hopping amplitudes between sites in SSH model) but when being integrated result in the same integer value W_n (like the genus of a manifold and its Gaussian curvature).

However, the invariance of W_n will only remain to be valid as long as the continuous modification of Hamiltonian parameters is carried out adiabatically¹, ensuring that our system remains in its ground state during the transition. Therefore, we need an energy gap that limits how slow the adiabatic process is performed. It follows then that to connect two topologically different insulators (with different W_n) the energy gap must be closed at some moment of the transition: we need to pass through a metallic phase, in order to change the topological index of our insulator. This process of changing the index W_n is what defines a topological phase transition. The topological equivalence between insulators is established when we can find an adiabatic path with a finite energy gap (such that W_n is conserved) connecting the two insulating phases.

We will demonstrate the consequences of this topological order in 1D and 2D materials by using two examples. The first of them (for 1D systems) will be the SSH model^{2,3}(sec. II). In this model, we will show a physical trait of topological insulators: the presence of edge states (located at the limits of a finite 1D chain⁴). The topologically trivial insulating phase will not possess such edge states(see FIG.1,2,6).



FIG. 1: Schematic representation of a finite chain in the SSH model. If we restrict the electron hopping allowing only B to A movement, 2 edge sites will be left isolated: zero-energy edge states localized at the A and B limits of the chain will appear.

In 2D systems, we will use a graphene honeycomb with the Haldane model⁵ as an example (sec.III). Its importance lies in the possibility of having quantized Hall conductance σ_{xy} , without the need of using a magnetic field (QAH phase)⁶ and as in the 1D system, edge states. These have a chiral character that prevents backscattering, producing a perfect edge conductance⁶ in one possible direction. σ_{xy} can be calculated using the Chern number (2) and the TKNN formula⁷:

$$\sigma_{xy} = \frac{e^2}{h} W_n \quad (3)$$

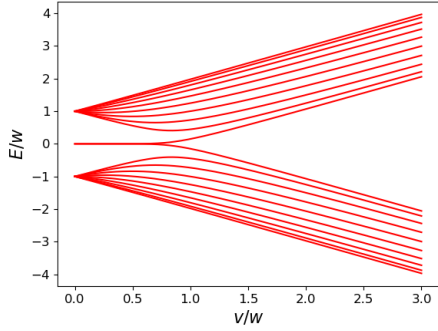


FIG. 2: Energies as a function of v/w for a finite chain of 10 dimers. As v/w grows, edge states get delocalised throughout the chain. The two-fold degeneracy when $E/w = 0$ is given by symmetric and anti-symmetric edge states.



FIG. 3: 1D chain in the SSH model. A sites form a Bravais lattice with parameter a . We are interested in the bulk properties, so we will consider periodic boundary conditions.

II. SSH MODEL

This model gives some insights into topological phases and how spin-less electrons hop between the sites of a 1D chain. The chain has N dimers, each one with two sites: A and B (see FIG.3). For reasons that we will see later, only one electron per unit cell is considered (this way, the chain will behave as an insulator). Electrons are only allowed to hop towards first neighbours. We will also neglect interactions between electrons, studying the many-body system in terms of a TB single particle Hamiltonian:

$$H = v \sum_{n=1}^N (|n, A\rangle \langle n, B|) + w \sum_{n=1}^{N-1} (|n+1, A\rangle \langle n, B|) + h.c. \quad (4)$$

We use a single orbital basis: $\{|n, l = A, B\rangle\}$. v and w are real and positive, we can always make this choice by an appropriate phase change on each $|n, A\rangle$ and $\langle n, B|$ states⁸. Since we are treating the bulk part of the chain, we have discrete translational symmetry, and we can apply the Bloch theorem. H is block diagonalised as a function of k (in the BZ), by performing a Fourier transform in the external Hilbert space⁸:

$$|n, l = A, B\rangle = \frac{1}{\sqrt{N}} \sum_{k \in \text{BZ}} e^{ikna} |k, l = A, B\rangle \quad (5)$$

Using the new basis ($\{|k, l = A, B\rangle\}$) of plane waves, the Bloch Hamiltonian is:

$$H(k) = \begin{pmatrix} 0 & v + we^{ika} \\ v + we^{-ika} & 0 \end{pmatrix} \quad (6)$$

The diagonal terms in (6) are zero because on-site potentials are set to zero. We can extract information about the band structure of the system diagonalizing $H(k)$. Its eigenvalues as a function of k are (see FIG.4):

$$E_{\pm}(k) = \pm \sqrt{v^2 + w^2 + 2vw \cos(ka)} \quad (7)$$

The eigenvectors are:

$$|k_{\pm}\rangle = \frac{1}{\sqrt{2}} \begin{pmatrix} \pm e^{-i\phi(k)} \\ 1 \end{pmatrix} \quad (8)$$

$$\phi(k) = \arctan\left(\frac{w \sin(ka)}{v + w \cos(ka)}\right) \quad (9)$$

A. Berry phase as a topological index for SSH model

Now we can use the tools presented in section I (Berry connection and curvature) to characterize the different insulating phases. We start with the SSH model. The Hamiltonian (6) should be rewritten in terms of the Pauli matrices:

$$H(\vec{k}) = \vec{d}(\vec{k}) \cdot \sigma \quad (10)$$

$$\vec{d}(k) = (v + w \cos(ka), w \sin(ka), 0) \quad (11)$$

Using the parameters v and w we can control smooth transitions between insulating phases. In the case of the SSH model, the closures are produced at the boundaries of the BZ (using (7)):

$$E_{\pm}(\pm \frac{\pi}{a}) = \pm \sqrt{(v-w)^2} = 0$$

Then, the condition to pass through the metallic phase is $v = w$ (see FIG.4). We can check the values of W_n for each insulating phase, and see which one of them is topological. The Berry connection for the lower band states $|k_{-}\rangle$ is:

$$A_{-}(k) = \langle k_{-} | i \frac{d}{dk} | k_{-} \rangle = \frac{1}{2} \frac{d\phi}{dk} \quad (12)$$

And (1) becomes:

$$W = \frac{1}{2\pi} \int_{-\pi}^{\pi} \frac{w^2 + vw \cos(x)}{v^2 + w^2 + 2vw \cos(x)} dx \quad (13)$$

Where $x = ka$. The integral (13) can be understood as a winding number. If we make the substitution $z = v + we^{ix}$ with $x \in [-\pi, \pi]$ in the formula for the winding number of a curve C in the complex plane:

$$W = \frac{1}{2\pi i} \oint_C \frac{1}{z} dz \quad (14)$$

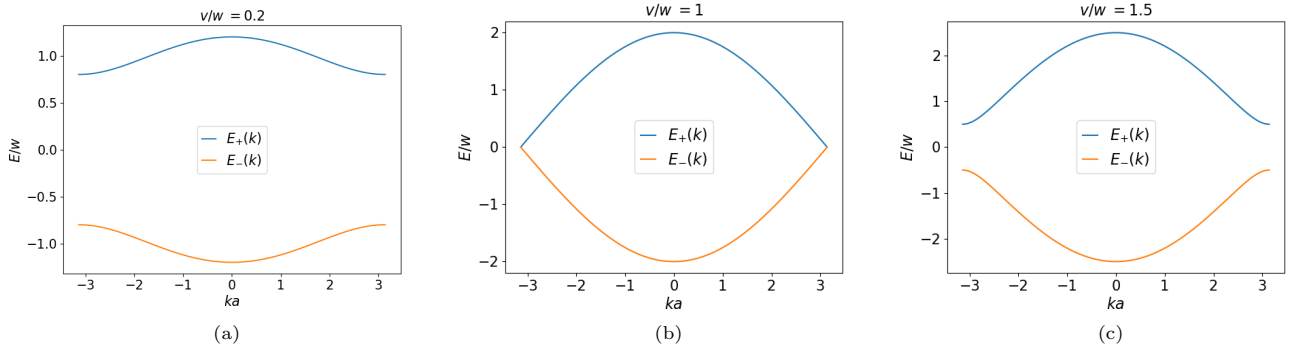


FIG. 4: Different dispersion relations corresponding to a transition from $v/w < 1$ to $v/w > 1$ in the SSH model. When $v/w \neq 1$, the bulk behaves as an insulator: the lower band is completely filled, the upper band is empty, and there is an energy gap.

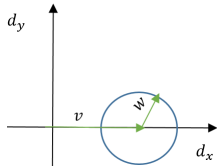


FIG. 5: Circle C parametrized with (11). The winding number in this case would be zero, because the circle does not enclose the origin.

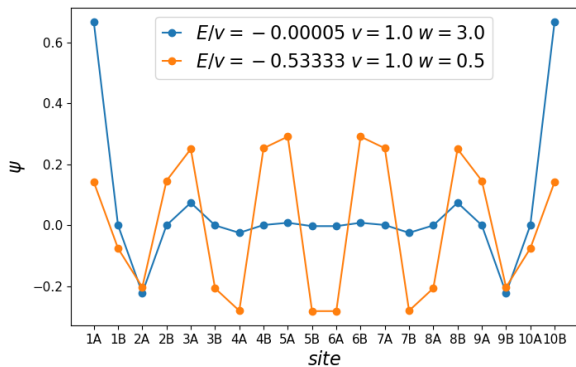


FIG. 6: Eigenstates in a finite chain of 10 dimers. The state with energy closest to zero in the trivial case is not an edge state (orange). Dots are only joined for visualization, the x axis is used to represent each element of the site basis.

we get:

$$W = \frac{1}{2\pi} \int_{-\pi}^{\pi} \frac{w^2 + v w \cos(x) + i v w \sin(x)}{v^2 + w^2 + 2v w \cos(x)} dx \quad (15)$$

The real part of (15) is (13), and its imaginary part vanishes for being the integral of an odd function on a symmetric interval. Taking \vec{d} as the parametrization of a circle: the case $v > w$ is a trivial insulator, and $v < w$ is topological (see FIG.2,6,5). The only way of changing the winding number is going through the origin ($v = w$ when crossing, a metallic phase).

III. HALDANE MODEL

The Haldane model⁵ is also based on tight-binding, but it has second neighbour hoppings (which are complex). We denote the first neighbour hopping by t_1 , the second neighbour hopping is equal to it_2 or $-it_2$ depending on the orientation in which we are hopping inside an hexagon cell (see FIG.7). The TB Hamiltonian can be written in general as:

$$H = \sum_{\vec{R}, \vec{R}', a, b} H_{ab}(\vec{R}, \vec{R}') |\vec{R}, a\rangle \langle \vec{R}', b| \quad (16)$$

Where \vec{R}, \vec{R}' are summed over all lattice sites, and a, b are summed over the A, B unit cell sites. $H_{ab}(\vec{R}, \vec{R}')$ are the hopping amplitudes for each pair of interacting sites in the lattice. Following the same procedure as with the SSH chain, we use the Bloch theorem and describe the problem in terms of plane waves. The 2×2 Bloch Hamiltonian is:

$$H(\vec{k}) = \begin{pmatrix} g(\vec{k}) & f(\vec{k}) \\ f^*(\vec{k}) & -g(\vec{k}) \end{pmatrix} \quad (17)$$

The first neighbour hopping is encoded in the f functions:

$$f(\vec{k}) = t_1 \left[1 + e^{-i\vec{k} \cdot \vec{a}_1} + e^{-i\vec{k} \cdot \vec{a}_2} \right] \quad (18)$$

$$g(\vec{k}) = \frac{\Delta_0}{2} + 2t_2 \left(\sin(\vec{k} \cdot \vec{a}_1) - \sin(\vec{k} \cdot \vec{a}_2) - \sin(\vec{k} \cdot (\vec{a}_1 - \vec{a}_2)) \right) \quad (19)$$

The function $g(\vec{k})$ has a finite mass term Δ_0 and is finite at the K and K' Dirac points where $f(K) = f(K') = 0$, with the property $g(K) = -g(K')$. Therefore, the gap has an *opposite sign* at K and K' . Band structure (see FIG.8) is given by:

$$E_{\pm}(\vec{k}) = \pm \sqrt{|f(\vec{k})|^2 + g^2(\vec{k})} \quad (20)$$

and eigenstates:

$$|\vec{k}_{\pm}\rangle = c_{\pm} \begin{pmatrix} 1 \\ \frac{E_{\pm}(\vec{k}) - g(\vec{k})}{f(\vec{k})} \end{pmatrix} \quad (21)$$

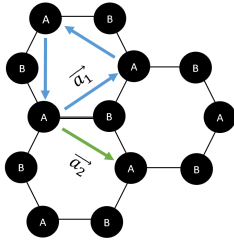


FIG. 7: Inside each honeycomb sublattice, counter-clockwise hopping is equal to it_2 (blue arrows). Clockwise hopping is $-it_2$ (green arrow). We use \vec{a}_1 and \vec{a}_2 as basis vectors.

$$t_2/t_1 = 0.092 \quad \Delta_0/t_1 = 0.8$$

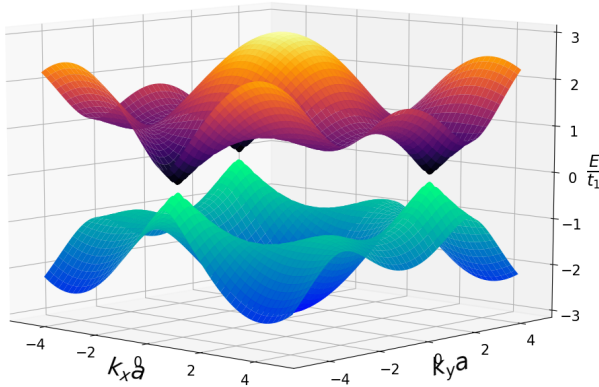


FIG. 8: Energy bands from (20) for graphene. We can see that three of the Dirac points have almost zero gap.

with c_{\pm} such that $\langle k_{\pm} | k_{\pm} \rangle = 1$

A. Chern number as a topological index for Haldane model

As with the SSH model, we look for transition points. We need relations between Δ_0 and t_2 at the Dirac points K and K' . We have:

$$\begin{aligned} \vec{a}_1 &= \frac{a}{2} (\sqrt{3}, 1) \\ \vec{a}_2 &= \frac{a}{2} (\sqrt{3}, -1) \end{aligned} \quad (22)$$

It will be convenient to define the coordinates:

$$\begin{aligned} \phi_1 &\equiv \vec{k} \cdot \vec{a}_1 = \frac{a}{2} (\sqrt{3}k_x + k_y) \\ \phi_2 &\equiv \vec{k} \cdot \vec{a}_2 = \frac{a}{2} (\sqrt{3}k_x - k_y) \end{aligned} \quad (23)$$

The Dirac points satisfy $f(K) = f(K') = 0$. In the phase

representation this means:

$$[1 + e^{i\phi_1} + e^{i\phi_2}] = 0 \quad (24)$$

or

$$1 + \cos \phi_1 + \cos \phi_2 = 0$$

$$\sin \phi_1 + \sin \phi_2 = 0$$

From the second equation, we choose $\phi_1 + \phi_2 = 0$. Using the fact that \cos is an even function, the first equation reads $1 + 2 \cos \phi_1 = 0$ or $\phi_1 = \frac{2\pi}{3}$ and $\phi_2 = -\frac{2\pi}{3}$. This gives the first Dirac point:

$$(K_x, K_y) = \left(0, \frac{4\pi}{3a}\right) \quad (25)$$

Now, we know this point occupies one corner in an hexagon. Its opposite should belong to the other sublattice:

$$(K'_x, K'_y) = \left(0, -\frac{4\pi}{3a}\right) \quad (26)$$

We use both points to get the transition condition ($g(\vec{k}) = 0$) on each sublattice of Dirac points K and K' (the condition is equivalent for all Dirac points belonging to the same sublattice):

- $K' : \frac{t_2}{\Delta_0} = \frac{1}{6\sqrt{3}} \approx 0.11785$
- $K : \frac{t_2}{\Delta_0} = \frac{1}{-6\sqrt{3}} \approx -0.11785$

The Chern number (2) should change as we vary the quotient t_2/Δ_0 . To calculate it we need the Berry curvature, which is defined as the rotational of the Berry connection:

$$\vec{\Omega}_n(\vec{k}) = \nabla_{\vec{k}} \times \langle n(\vec{k}) | i \nabla_{\vec{k}} | n(\vec{k}) \rangle \quad (27)$$

A useful formula was derived by Berry¹:

$$\vec{\Omega}_n(\vec{k}) = \text{Im} \sum_{m \neq n} \frac{\langle n(\vec{k}) | \nabla_{\vec{k}} H(\vec{k}) | m(\vec{k}) \rangle \times \langle m(\vec{k}) | \nabla_{\vec{k}} H(\vec{k}) | n(\vec{k}) \rangle}{(E_m(\vec{k}) - E_n(\vec{k}))^2} \quad (28)$$

We use this expression to calculate numerically the integral (2). In FIG.9 we see the results: on each transition the gap closings change W , creating two topologically distinct phases when $t_2/\Delta_0 < -0.11785$, and $t_2/\Delta_0 > 0.11785$. W is zero when the Berry curvature has opposite signs at the Dirac points K and K' .

IV. CONCLUSIONS

We have seen the consequences of topological order in different materials by checking the integer variation of W_n . The SSH model presented one bulk topological phase, with symmetric and antisymmetric edge states at

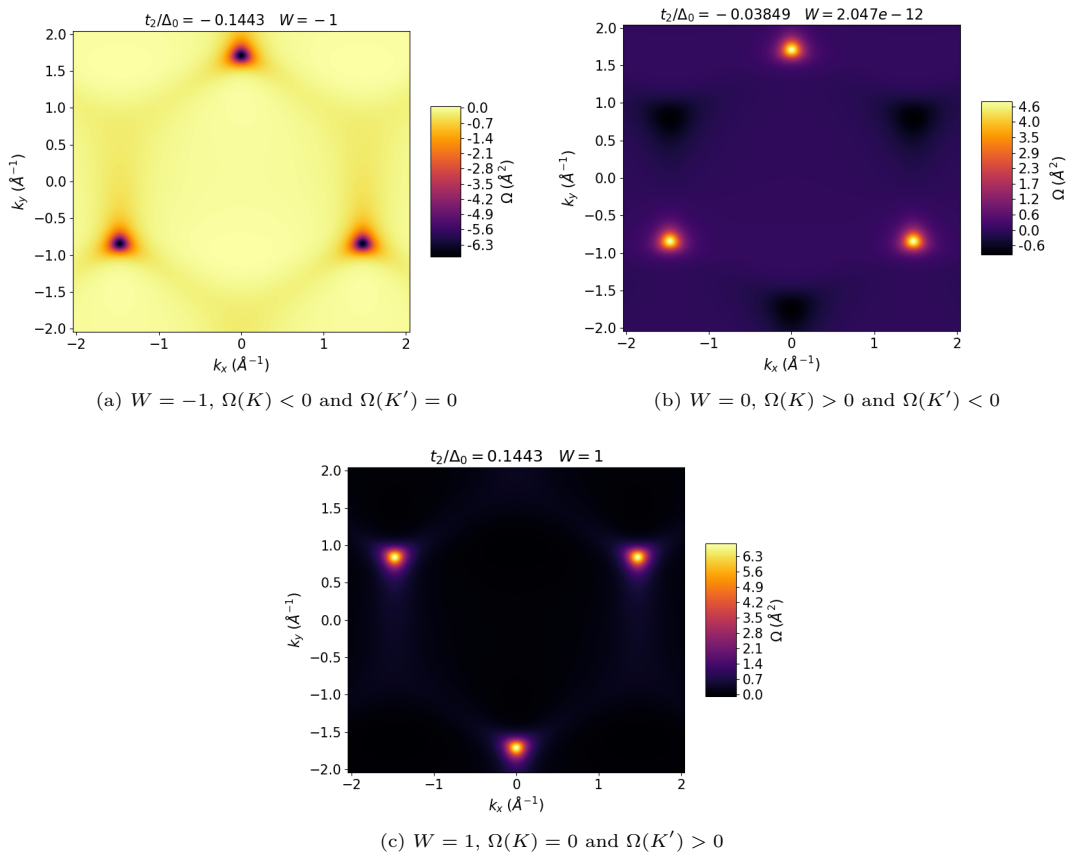


FIG. 9: Contour plots of Ω for the lowest energy band in Haldane's graphene.

the boundaries. In the Haldane example, we have shown that it is possible to produce topological phases (and quantized Hall effect) without the need of a magnetic field. Moreover, Haldane's model also provided two topologically different insulating phases, as a consequence of the multiple possibilities of band closing at the Dirac points (see FIG.8). These phases have edge states associated as in the SSH model⁹. We have seen then that there are quantized properties in macroscopic materials, which have physically measurable consequences, and are

related to topological phase transitions.

V. ACKNOWLEDGEMENTS

I would like to show my gratitude to the GEFES for giving me this opportunity. Also to my supervisor, Joaquín Fernández Rossier, for the great work he has done guiding me in this completely new topic for me.

¹ M. V. Berry, Proc. R. Soc. London, Ser. A 392, 45 (1984)

² W. P. Su, J. R. Schrieffer, and A. J. Heeger, Physical Review Letters 42 (1979)

³ W. P. Su, J. R. Schrieffer, and A. J. Heeger, Physical Review B 22 (1983)

⁴ Delplace, P., D. Ullmo, and G. Montambaux., Physical Review B 84.19 (2011)

⁵ Haldane, F. D. M., 1988, Phys. Rev. Lett.61 (2015)

⁶ Lado, J.L., N. García-Martínez, and J. Fernández-Rossier,

Synthetic Metals 210 (2015): 56-67.

⁷ D. J. Thouless, M. Kohmoto, M. P. Nightingale, and M. den Nijs, Physical Review Letters, Vol. 49, No. 6, pp. 405-408 (1982).

⁸ Janos K. Asboth, et. al. 'A Short Course on Topological Insulators' (Springer, 2016).

⁹ Hao, Ningning and Zhang, Ping and Wang, Zhigang and Zhang, Wei and Wang, Yupeng, Physical Review B, Vol.78, No.7, (2008)